Design and Comparison of Vernier Permanent Magnet Machines

S. L. Ho, Shuangxia Niu, and W. N. Fu

Department of Electrical Engineering, The Hong Kong Polytechnic University, Hong Kong

Vernier permanent magnet (VPM) machines can be utilized for direct drive applications by virtue of their high torque density and high efficiency. The purpose of this paper is to develop a general design guideline for split-slot low-speed VPM machines, generalize the operation principle, and illustrate the relationship among the numbers of the stator slots, coil poles, permanent magnet (PM) pole pairs, thereby laying a solid foundation for the design of various kinds of VPM machines. Depending on the PM locations, three newly designed VPM machines are reported in this paper and they are referred to as 1) rotor-PM Vernier machine, 2) stator-tooth-PM Vernier machine, and 3) stator-yoke-PM Vernier machine. The back-electromotive force (back-EMF) waveforms, static torque, and air-gap field distribution are predicted using time-stepping finite element method (TS-FEM). The performances of the proposed VPM machines are compared and reported.

***Index Terms*—Direct drive, electric motor, finite element method (FEM), permanent magnet (PM), time stepping, Vernier.**

I. Introduction

With a growing concern about fossil fuel depletion and environmental pollution crises, electric propulsion systems are increasingly being used in motorcycles, automobiles, trains, vessels, and as generators for wind turbines. Low-speed direct-drive gearless machines are more meritorious than their high-speed counterparts with gear boxes because the former have no associated gear and no related problems such as oil maintenance, noise issue, losses, and so on. However, conventional direct-drive machines suffer from bulkiness and low efficiency. Vernier permanent magnet (VPM) machines which exploit magnetic gear effects to modulate the magnetic fields are capable of producing high torque at a relatively low speed [1], [2]. Due to their structural compactness, high torque density, and high efficiency, VPM machines are desirable for direct-drive applications [3], [4].

Previous literatures only focus on individual structures of VPM machines [1]–[5]. This paper aims to develop a general design guideline for split-slot low-speed VPM machines, generalize the operation principle, and illustrate the relationship among the stator slot number, stator winding pole number, permanent magnet (PM) number, thereby laying a foundation for the design of various kinds of VPM machines. Based on PM locations, the three newly designed VPM machines being studied in this paper are referred to as 1) rotor-PM Vernier machine, 2) stator-tooth-PM Vernier machine, and 3) stator-yoke-PM Vernier machine. To reduce the slot number and reduce the end windings, which in turn reduces the copper loss, the stator windings are designed as concentrated windings. To realize low operating speed under limited frequency, the pole number needs to be large. In this paper, each stator tooth is split into several fake slots to produce multipole effect. To increase the air-gap diameter and obtain high torque, all of the VPM machines are designed with an outer rotor structure. To allow a fair comparison, the outer diameter, air-gap diameter and stack length of all the three motors are the same.

Time-stepping finite element method (TS-FEM) has been successfully used in the analysis of the transient and static performance of electric machines. The FEM model takes into account the effects of saturation, eddy current, and the mechanical movement of rotor [6]. In this paper, the TS-FEM is used to analyze and compare the performance of these proposed VPM machines. The steady-state and transient performances including cogging torque and back-electromotive force (back-EMF) of the machine are simulated and analyzed.

II. Principle of Operation

A. Principle of Operation

For VPM machines, their principle of operation is based on the "magnetic gear effect." In magnetic gears (MGs), the low-speed multipole-pair and high-speed machine with fewer PM pole pairs on the two rotating parts can be magnetically coupled with one another through their flux modulating ferrite poles. The relative movement between the permeance and the magnetomotive force (MMF) of PMs gives rise to the desired flux variation. A small movement of the low-speed PMs results in a large change in the flux, and the flux rotation can interact with the fast-speed MMF of the PMs to rotate at the same synchronous speed [7]. Based on this principle, the high-speed low-torque output can be transferred through a specific gear ratio to the multipole PMs on the rotor to give rise to low speed and high torque.

In VPM machines, the basic principle is the same, which means the MMF created by PMs is modulated by the air-gap permeance and hence a desired fast flux variation is produced. The major difference is that the high-speed MMF is produced by the steady stator windings rather than by the PMs. Based on such operation principles, different types of VPM machines can be designed. The PMs may be carried by the rotor and the stator teeth can be split into several fake teeth to serve as the flux modulating poles, which changes only in the circumferential direction. Another version of VPMs is that the PMs are designed to be carried by the stator and the salient poles are carried by the rotor to produce the variable air-gap permeance. The PMs can be surface mounted on the stator teeth or be inset into the stator yokes. Although many VPM machine designs have emerged,

Manuscript received February 20, 2011; accepted May 15, 2011. Date of current version September 23, 2011. Corresponding author: W. N. Fu (e-mail: eewnfu@polyu.edu.hk).

Color versions of one or more of the figures in this paper are available online at http://ieeexplore.ieee.org.

Digital Object Identifier 10.1109/TMAG.2011.2157309

there are very few detailed instructions in the determination of the necessary relations among the stator and rotor teeth as well as on the PM and armature winding polarities so as to synchronize the rotor speed to produce useful torque. The purpose of this paper is to determine the relation among various design values to allow the synchronous operation of the VPM machines to be realized.

B. Generic Analysis of VPMs

To analyze VPMs, the magnetic resistance and saturation of the steel parts are assumed to be negligible. The MMF of the PMs can be expressed as

$$F(\theta) = \sum_{m=1,3,5,\ldots}^{\infty} \frac{F_{\rm PM}}{m} cos\left[\frac{2m\pi}{\theta_{\rm PM}}(\theta - \varepsilon\omega_r t)\right] \quad (1)$$

where θ is the stator position, ω_r is the rotor speed, $\theta_{\rm PM}$ is the angular width of one pair of PMs, and $F_{\rm PM}$ is the amplitude of the fundamental component of F. With PMs on stator, $\varepsilon = 0$; and with PMs on rotor, $\varepsilon = 1$. Neglecting the higher order components, the MMF of the PMs can be expressed as

$$F(\theta) \approx F_{\rm PM} cos\left(\frac{2\pi}{\theta_{\rm PM}}(\theta - \varepsilon\omega_r t)\right). \quad (2)$$

If toothed structure is only designed on the stator, the permeance coefficient due to the stator is expressed as

$$P_s(\theta) = P_{s\_0} + \sum_{m_s=1}^{\infty} P_{s\_1} cos\left(\frac{2m_s\pi}{\theta_s}\theta\right) \quad (3)$$

where θ_s is the angular width of each stator slot pitch, and P_{s_1} is the amplitude of the fundamental component of P_s.

Neglecting the higher order components, the MMF of the stator permeance coefficient can be expressed as

$$P_s(\theta) \approx P_{s\_0} + P_{s\_1} cos\left(\frac{2\pi}{\theta_s}\theta\right). \quad (4)$$

If toothed structure is only designed on the rotor, the permeance coefficient due to the stator is expressed as

$$P_r(\theta) = P_{r\_0} + \sum_{m_r=1}^{\infty} P_{r\_1} cos\left(\frac{2m_r\pi}{\theta_r}(\theta - \omega_r t)\right) \quad (5)$$

where θ_r is the angular width of each rotor slot pitch, and P_{r_1} is the amplitude of the fundamental component of P_r. Neglecting the higher order components, the MMF of the rotor permeance coefficient is

$$P_r(\theta) \approx P_{r\_0} + P_{r\_1} cos\left(\frac{2\pi}{\theta_r}(\theta - \omega_r t)\right). \quad (6)$$

If toothed structure is designed both on the rotor and the stator, the fundamental component of the permeance coefficient due to both salient teeth is expressed as [8]

$$\begin{aligned} P_{rs}(\theta) \approx P_{rs0} \Bigg\{ & 1 + \frac{P_{r\_0}P_{s\_0}}{2P_{rs0}^2} \\ & \times \left\{ cos\left[\left(\frac{2\pi}{\theta_r} - \frac{2\pi}{\theta_s}\right)\theta - \frac{2\pi\omega_r t}{\theta_r}\right] \right. \\ & \left. + cos\left[\left(\frac{2\pi}{\theta_r} + \frac{2\pi}{\theta_s}\right)\theta - \frac{2\pi\omega_r t}{\theta_r}\right] \right\} \\ & + \frac{P_{s1}}{P_{rs0}} cos\left(\frac{2\pi}{\theta_s}\theta\right) \\ & + \frac{P_{r1}}{P_{rs0}} cos\left(\frac{2\pi}{\theta_r}(\theta - \omega_r t)\right) \Bigg\} \end{aligned} \quad (7)$$

where P_{rs0} is the fundamental component amplitude of P_{rs}.

C. Specific VPM Structure Analysis

For machines with PMs on rotor and salient poles on stator, the air-gap magnetic flux density can be expressed as

$$\begin{aligned} B_{\rm PM} &= F(\theta)P_s(\theta) \approx B_{s1}(\theta) + B_{s1\_h}(\theta, t) \\ &\approx B_{s1} cos\left(\frac{2\pi}{\theta_{\rm PM}}(\theta - \omega_r t)\right) \\ &\quad + B_{s1\_h} cos\left(\left(\frac{2\pi}{\theta_{\rm PM}} - \frac{2\pi}{\theta_s}\right)\theta - \frac{2\pi}{\theta_{\rm PM}}\omega_r t\right) \end{aligned} \quad (8)$$

where $B_{s1} = F_{\rm PM}P_{s\_0}$ and $B_{s1\_h} = F_{\rm PM}P_{s\_1}/2$. To synchronize the rotor speed to produce a useful torque, the number of pole pairs of the stator windings p must be equal to the number of the pole pairs of the space harmonic. It can be expressed as

$$p = |z_{pm} - z_s|. \quad (9)$$

The corresponding rotational velocity of the flux density space harmonics is given by

$$|\omega| = z_{pm}\omega_r \quad (10)$$

where $z_{pm} = 2\pi/\theta_{pm}$ and $z_r = 2\pi/\theta_r$.

For machines with PMs on stator and salient poles on rotor, the air-gap magnetic flux density can be expressed as

$$\begin{aligned} B_{\rm PM} &= F(\theta)P_r(\theta) \approx B_{r1}(\theta) + B_{r1\_h}(\theta, t) \\ &\approx B_{r1} cos(z_{pm}\theta) + B_{r1\_h} cos\left((z_{pm} - z_r)\theta + z_r\omega_r\right) \end{aligned} \quad (11)$$

where $B_1 = F_{\rm PM}P_{r\_0}$ and $B_{1\_h} = F_{\rm PM}P_{r\_1}/2$. The number of pole pairs of the stator windings p can be expressed as

$$p = |z_{pm} - z_s|. \quad (12)$$

The corresponding rotational velocity of the flux density space harmonics is given by

$$|\omega| = z_r\omega_r. \quad (13)$$

For machines with PMs on stator and salient poles on both rotor and stator, the air-gap magnetic flux density can be expressed as

$$\begin{aligned} P_{rs}(\theta) \approx & F_{pm}P_{rs0} \\ & \times \Bigg\{ cos(z_{pm}\theta) + \frac{P_{s1}}{P_{rs0}} cos(z_s\theta) cos(z_{pm}\theta) \\ & + \frac{P_{r\_0}P_{s\_0}}{4P_{rs0}^2} \left\{ cos\left[(z_{pm} + z_r - z_s)\theta - z_r t\right] \right. \\ & \quad + cos\left[(z_{pm} - z_r + z_s)\theta + z_r t\right] \\ & \quad + cos\left[(z_{pm} + z_r + z_s)\theta - z_r t\right] \\ & \quad \left. + cos\left[(z_{pm} - z_r - z_s)\theta + z_r t\right] \right\} \\ & + \frac{P_{r1}}{4P_{rs0}} \left(cos\left((z_{pm} + z_r)\theta - z_r t\right) \right. \\ & \quad \left. + cos\left((z_{pm} - z_r)\theta + z_r t\right) \right) \Bigg\} \end{aligned} \quad (14)$$

where $z_s = 2\pi/\theta_s$. Since z_s is chosen to be close to z_r (such as in Machine III, $z_s = 36$ and $z_r = 32$), then by neglecting the high harmonic components, p can be given as

$$p = |z_{pm} \pm (z_r - z_s)|. \quad (15)$$

The corresponding rotational velocity of the flux density space harmonics is given by

$$|\omega| = z_r\omega_r. \quad (16)$$

D. Proposed Machine Structure of VPMs

The machines to be investigated are depicted in Figs. 1–3. The basic specifications of the machines are identical to allow

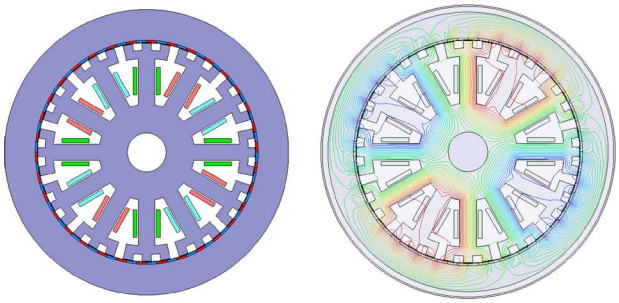

(a) (b)

Fig. 1. Machine I. (a) Structure. (b) Flux line distributions.

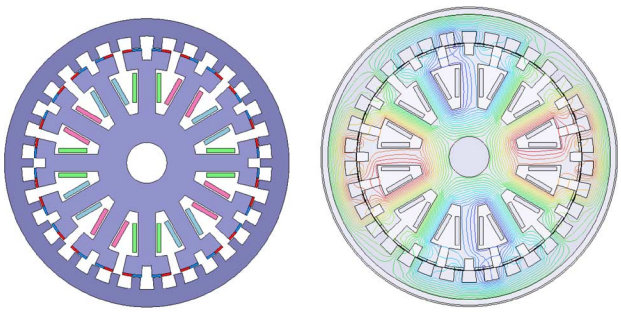

(a) (b)

Fig. 2. Machine II. (a) Structure. (b) Flux line distributions.

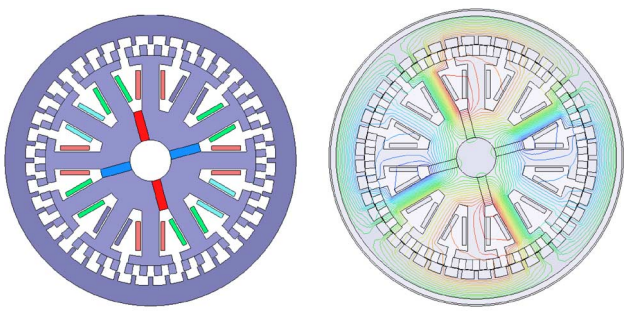

(a) (b)

Fig. 3. Machine III. (a) Structure. (b) Flux line distributions.

a fair comparison. For example, the outer diameter is 200 mm; the air-gap radius is 79.3 mm; the stator slot number is 12; the stator windings are designed with three phases; the conductor number of each coil is 20; the phase current is 30 A; the air-gap length is 0.6 mm; and the stack length is 65 mm.

When PMs are carried by the stator, the stator slot openings may influence the harmonic components of the MMF distributions of the magnets. However, it does not influence the fundamental harmonic components of the PMs. In Machine II, the slot openings give rise to a reduction in PM MMF. Fig. 4 shows the harmonic order with the highest amplitude is the ninth, which is the same with Machine I.

Machine I: The rotor-PM Vernier machine has 34 surface mounted PM pole pairs on the rotor iron core, 12 stator slots. Each stator tooth is split into three fake teeth serving as a flux modulating pole. The PM pole-pair number $z_{pm} = 34$ which is very close to stator fake tooth number $z_s = 36$. According to (9), the working flux produced by the stator windings has $p = 2$ pole pairs.

Machine II: The stator-tooth-PM Vernier machine, as one kind of flux reversal machines [5], has 24 surface mounted PM

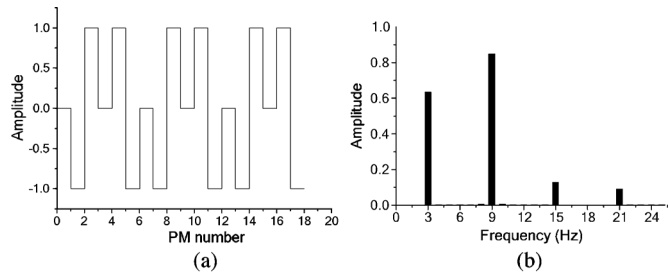

(a) (b)

Fig. 4. PM MMF waveforms and spectrum for Machine II. (a) MMF waveforms. (b) Spectrum.

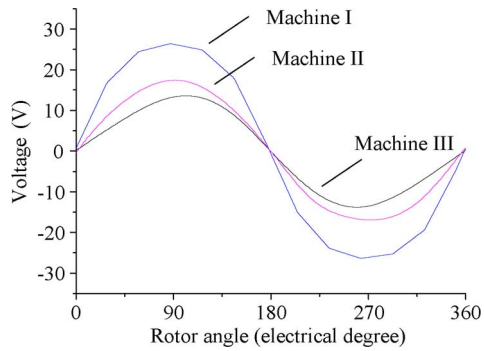

Fig. 5. Comparison of back-EMF waveforms.

pole pairs on the stator tooth. In this machine, each stator tooth is split by one slot and the stator slot pole-pair number is 12. The pole-pair number of the rotor is 34. According to (12), the working flux has $p = 2$ pole pairs.

Machine III: The stator-yoke-PM Vernier machine, as one kind of double salient machines, has $z_s = 48$ stator teeth and $z_r = 44$ rotor teeth. The PM pole-pair number is $z_{pm} = 2$. According to (15), the pole-pair number of the working flux is $p = 2$ pole pairs.

III. Finite Element Analysis

As shown in Figs. 1–3, the working flux distributions show that the three VPM machines can work well with a two-pole-pair stator winding in their full load operation. The two-pole-pair stator winding frequency for Machines I and II is 136 Hz, which synchronizes with the rotor with 34 poles to rotate at 240 r/min. For Machine III, the frequency is 176 Hz with a rotor speed of 240 r/min, which is consistent with the operation principle analysis as described in Section II.

The back-EMF waveforms are given in Fig. 5, and it can be seen that back-EMF of Machine I is sinusoidal and significantly higher than those of Machines II and III. The open-circuit air-gap flux density distribution is shown in Fig. 6. Since the PM position and salient structures are not the same, the flux distributions are also quite different. However, each air-gap flux density distribution has a second-order space harmonic to react with their two-pole-pair stator windings.

The torque density varies with different thickness of the PMs. Fig. 7 shows the variation of the maximum torque with the radial thickness of PM in Machine I. It can be seen that an optimum thickness of the PMs results in maximum torque transmission. The optimum thickness of PM in Machines I, II, and III are 1.87, 1.55, and 3.5 mm, respectively. Machine I has the largest PM material utilization. With the optimized thickness of

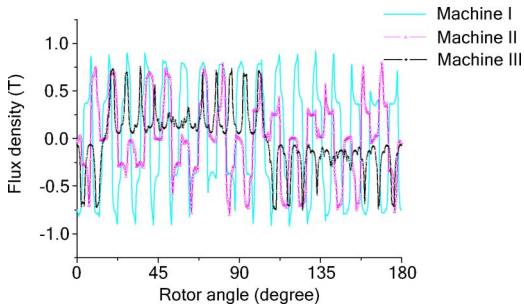

Fig. 6. Comparison of air-gap field distribution.

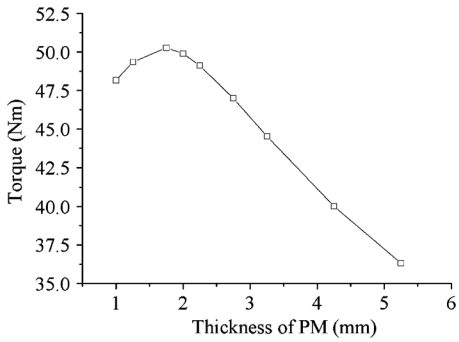

Fig. 7. Variation of maximum torque with PM radial thickness in Machine I.

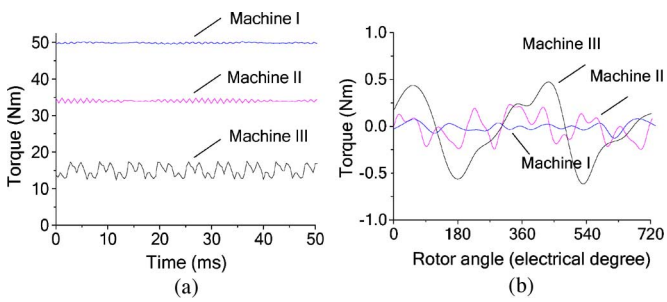

Fig. 8. Torque waveforms. (a) Full load torque at 240 r/min. (b) Cogging torque waveforms.

PM, the torque waveforms with the same loading current can be compared in Fig. 8(a). It can be seen that Machine I has the highest torque and since Machine III has a high armature reaction, its output torque is the lowest.

Cogging torque plays an important role in the operation of these machines and it affects the machine's self-starting ability, and produces noise and mechanical vibration. The cogging torque waveforms are compared in Fig. 8(b). It is shown that the torque ripples are relatively small compared with the rated output torque of these machines. The reason is that the cogging torque ripple is approximately related to the inverse of the smallest common multiple of the salient pole numbers or the PM pole number. Within the three machines, Machine I has the lowest cogging torque.

IV. Conclusion

In this paper, a general design guideline for split-slot low-speed VPM machines is developed, which illustrates the operation principle and the relationship among the stator slots, coil poles, and PM pole-pair number. Three VPM machines including rotor-PM Vernier machine, stator-tooth-PM Vernier machine, and stator-yoke-PM Vernier machine are designed and their back-EMF waveforms, static torque, and air-gap field distribution are predicted by TS-FEM. The TS-FEM analysis results agree well with the theoretical analysis. From the comparison results, the rotor-PM machine has the highest torque density and the lowest cogging torque and is a promising design for direct-drive applications. However, when considering the PM cost, the stator-tooth-PM Vernier machine uses the least PM materials when compared to its counterparts.

Acknowledgment

This work was supported by the Research Grant Council of the Hong Kong SAR Government under Projects PolyU 5176/09E and G-YX4B.

References

[1] E. Spooner and L. Hardock, "Vernier hybrid machines," *Inst. Electr. Eng. Proc. B—Electr. Power Appl.*, vol. 150, no. 6, pp. 655–662, Nov. 2003.

[2] A. Toba and T. A. Lipo, "Generic torque-maximizing design methodology of surface permanent-magnet vernier machine," *IEEE Trans. Ind. Appl.*, vol. 36, no. 6, pp. 1539–1546, Nov./Dec. 2000.

[3] S. Niu, S. L. Ho, W. N. Fu, and L. L. Wang, "Quantitative comparison of novel vernier permanent magnet machines," *IEEE Trans. Magn.*, vol. 46, no. 6, pp. 2032–2035, Jun. 2010.

[4] S. Niu, S. L. Ho, and W. N. Fu, "A novel direct-drive dual-structure permanent magnet machine," *IEEE Trans. Magn.*, vol. 46, no. 6, pp. 2036–2039, Jun. 2010.

[5] D. G. Dorrell, I. Chindurza, and F. Butt, "Operation, theory and comparison of the flux reversal machine—Is it a viable proposition?," in *Proc. 5th IEEE Int. Conf. Power Electron. Drive Syst.*, Nov. 2003, vol. 1, pp. 253–258.

[6] W. N. Fu, P. Zhou, D. Lin, S. Stanton, and Z. J. Cendes, "Modeling of solid conductors in two-dimensional transient finite-element analysis and its application to electric machines," *IEEE Trans. Magn.*, vol. 40, no. 2, pp. 426–434, Mar. 2004.

[7] K. Atallah, S. D. Calverley, and D. Howe, "Design, analysis and realization of a high-performance magnetic gear," *Inst. Electr. Eng. Proc. —Electr. Power Appl.*, vol. 151, no. 2, pp. 135–143, Mar. 2004.

[8] P. L. Alger, *The Nature of Polyphase Induction Machines*. New York: Wiley, 1951.